Proceedings of the ASME 2023
Pressure Vessels & Piping Conference
PVP2023
July 16-21, 2023, Atlanta, Georgia, USA

PVP2023-106413

FATIGUE CRACK INITIATION AND FATIGUE LIFE TESTING OF HIGH-STRENGTH AUSTENITIC STAINLESS STEEL TUBING WITH INTERNAL HYDROGEN

Chris San Marchi[1], Joseph A. Ronevich[1], Johan Pohl[2], Severin Ramseyer[2], Davide Cortinovis[2], Stefan Eckmann[3]

[1]Sandia National Laboratories, Livermore, CA, USA
[2]Endress + Hauser Flow AG, Reinach, Switzerland
[3]Fraunhofer Institute for Mechanics and Materials IWM, Freiburg, Germany

ABSTRACT

Austenitic stainless steels have been extensively tested in hydrogen environments; however, limited information exists for the effects of hydrogen on the fatigue life of high-strength grades of austenitic stainless steels. Moreover, fatigue life testing of finished product forms (such as tubing and welds) is challenging. A novel test method for evaluating the influence of internal hydrogen on fatigue of orbital tube welds was reported, where a cross hole in a tubing specimen is used to establish a stress concentration analogous to circumferentially notched bar fatigue specimens for constant-load, axial fatigue testing. In that study (Kagay et al, ASME PVP2020-8576), annealed 316L tubing with a cross hole displayed similar fatigue performance as more conventional materials test specimens. A similar cross-hole tubing geometry is adopted here to evaluate the fatigue crack initiation and fatigue life of XM-19 austenitic stainless steel with high concentration of internal hydrogen. XM-19 is a nitrogen-strengthened Fe-Cr-Ni-Mn austenitic stainless steel that offers higher strength than conventional 3XX series stainless steels. A uniform hydrogen concentration in the test specimen is achieved by thermal precharging (exposure to high-pressure hydrogen at elevated temperature for two weeks) prior to testing in air to simulate the equilibrium hydrogen concentration near a stress concentration in gaseous hydrogen service. Specimens are also instrumented for direct current potential difference measurements to identify crack initiation. After accounting for the strengthening associated with thermal precharging, the fatigue crack initiation and fatigue life of XM-19 tubing were virtually unchanged by internal hydrogen.

Keywords: Hydrogen Testing, Fatigue, High-Pressure

1. INTRODUCTION

As high-pressure hydrogen technologies become more ubiquitous, high-strength alternatives to conventional materials are needed. Type 316 austenitic stainless steels are the common benchmark for high-pressure tubing, valve blocks and component housings in gaseous hydrogen systems because of their superior resistance to hydrogen-assisted fatigue and fracture. However, 300-series austenitic stainless steels suffer from low strength, which prevents efficient, lightweight structures. Type XM-11 and XM-19 are nitrogen-strengthened Fe-Cr-Ni-Mn austenitic stainless steels that offer higher strength than common 300-series austenitic stainless steels and are potentially superior alternatives to 300-series alloys. The superior resistance of type 316 to hydrogen effects is often associated with its relatively high nickel content (10-14 wt%); often characterized as nickel equivalent. Type XM-19 austenitic stainless steel can be considered a derivative of type 316 with more than twice the nickel content of the XM-11 alloy; whereas the leaner XM-11 alloy can be considered a derivative of type 304L.

The microstructure of austenitic stainless steels can influence its performance in hydrogen environments [1]. Thus, the differences between the microstructure of the raw materials and the condition in the final product form should be carefully considered. For example, seamless tubing is generally manufactured from bar (large, welded pipe is manufactured from plate or coil) through deformation processes that significantly alter the microstructure of the tubing (relative to the starting bar). Here, the goal is to assess the fatigue response of XM-19 tubing for service in high-pressure gaseous hydrogen environments.

Fatigue testing of tubing for environmental compatibility is a challenging endeavor since it is difficult to simulate the service environment in a laboratory test. In this study, a novel axial loading method is used to evaluate the fatigue response of tubing

material. A cross hole (i.e., perpendicular to the tube axis) is machined in the middle of a length of tubing to promote failure. The cross hole induces a stress concentration that can be designed to be consistent with the circumferentially notched tensile configuration for wrought bar. Additionally, the fatigue response of orbital tube welds can be evaluated by centering the cross hole in a welded joint, as demonstrated in Ref. [2]. For austenitic stainless steels, the gaseous hydrogen environment is simulated by pre-saturating the test specimen with hydrogen, as described in previous work [3, 4].

While the influence of hydrogen on mechanical properties of XM-19 have been reported in the literature [5-9], hydrogen-assisted fatigue has not been studied for this alloy (see review in Ref. [10]). In this study, we report on the fatigue life of XM-19 austenitic stainless steel tubing with high concentration of internal H and consider the effect of multiple annealing steps on the fatigue response.

2. MATERIALS AND METHODS

Materials

High-pressure XM-19 tubing is the subject of this study. XM-19 is a high-strength austenitic stainless steel, also referred to as 22Cr-13Ni-5Mn (or simply 22-13-5) in the literature. The composition of the XM-19 tubing is provided in Table 1.

The tubing was provided in the solution-annealed condition with an outside diameter of 6.0 mm and an internal diameter of 3.6 mm. The as-received condition is referred to as condition 'A'. After cutting the tubing to specimen lengths, a batch of specimens was annealed at temperature of 1050˚C, referred to as condition 'B'. Condition 'C' experienced two annealing cycles at temperature of 1050˚C.

Environments

The internal hydrogen condition was achieved by thermal precharging in gaseous hydrogen at a pressure of 1,380 bar and a temperature of 300°C for sufficient time to achieve uniform saturation through the thickness of the tubing wall. A few days are needed for saturation of the 1.2mm wall thickness, but specimens were thermally precharged for about 10 days in this case. To prevent hydrogen loss after thermal precharging, specimens are stored at −50°C (223K) until testing. All testing was conducted in laboratory air at room temperature (20˚C). Non-precharged specimens are referred to as NP, whereas H-precharged specimens are referred to as PC.

Tensile and Fatigue Test Methods

Tensile and fatigue specimens were straight sections of tubing, nominally 100 mm long. Specimens were gripped with (manual) wedge grips over a length of approximately 25 mm, leaving a gauge section (distance between wedge grips) of 50 mm. Pins were inserted approximately 25 mm into the tubing ends prior to gripping to prevent collapse of the tubing in the wedge grips. For some fatigue tests, the tube ends were threaded for gripping in threaded grips. Both tensile and fatigue testing was conducted on standard servohydraulic load frames.

Tensile specimens consisted of straight sections of tubing without any special preparation (unlike the fatigue specimens). An extensometer with gauge length of 25.4 mm was attached to the middle of the tensile specimen to determine strain. Tensile tests were conducted at constant displacement of about 2.5 mm/min, corresponding to a nominal strain rate of 6×10^{-4} s^{-1}. The 0.2% offset yield strength (Sy), ultimate tensile strength, (Su), uniform elongation (Elu = engineering strain at peak load) and total elongation (Elt) are reported.

Fatigue test specimens utilized a stress concentration to initiate fatigue failure. The stress concentration consisted of a cross hole through both sides of the tubing at the mid-point of the specimen. The diameter of the hole was 1.7 mm, corresponding to an elastic stress concentration factor (K_t) of about 4. In the shorter fatigue tests, crack initiation at the cross holes was monitored using direct current potential difference (DCPD). A constant current of 1A was applied to the specimens through leads attached approximately 3 mm from the ends of the 100 mm long specimens; the current leads were spot welded diametrically opposite from one another (i.e., 180˚ apart around the circumference, but on opposite ends of the specimen length). The potential difference was monitored from connections approximately 3 mm from the center of the cross hole, longitudinally on either side of the hole (thus the distance between the voltage leads was about 6 mm). The voltage leads were attached to the specimen by welding the wire leads to cotter pins and clipping the pins to the tubular specimen at the specified location. Thermoelectric effects were minimized by current switching (polarization reversal) using a commercial fatigue control and monitoring system (from Fracture Technology Associates). Crack initiation is determined from the inflection of the voltage-cycle number curve, in the same way as described in Refs. [11, 12] for circumferentially notched tension (CNT) fatigue testing. Figure 1 shows examples of the potential difference signal and the point of crack initiation.

Load-control tension-tension fatigue tests were performed with a constant load cycle. A load ratio (R) of 0.1 was used for all tests. Most tests were conducted at frequency of 1 Hz, although a few tests were conducted at 10 or 80 Hz. The fatigue stress in this study is defined as the net-section stress across a plane at the center of cross hole (i.e., a plane representing the minimum cross-sectional area of the tube with a cross hole). The minimum cross-sectional area is assumed to be the same for all specimens and equivalent to 13.9 mm^2 (compared to the cross-sectional area of the tubing without the cross hole: 18.1 mm^2).

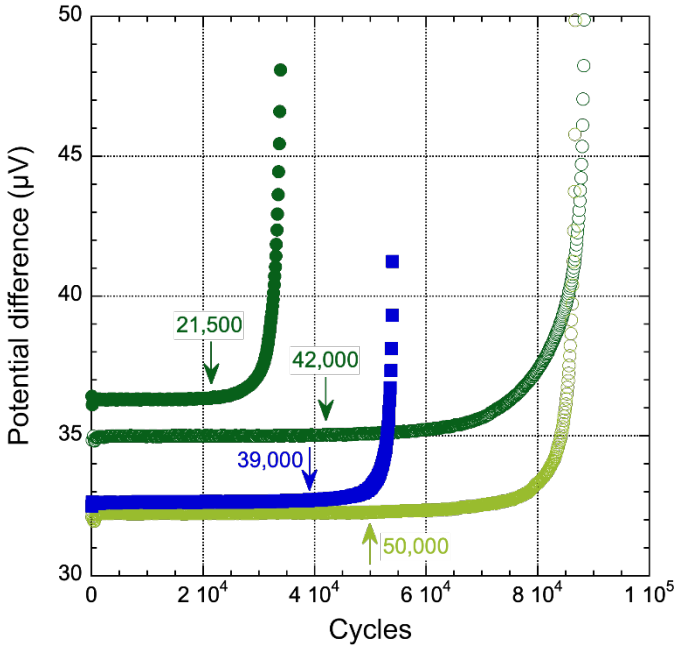

FIGURE 1: EXAMPLES OF POTENTIAL DIFFERENCE SIGNAL AND IDENTIFICATION OF CRACK INITIATION.

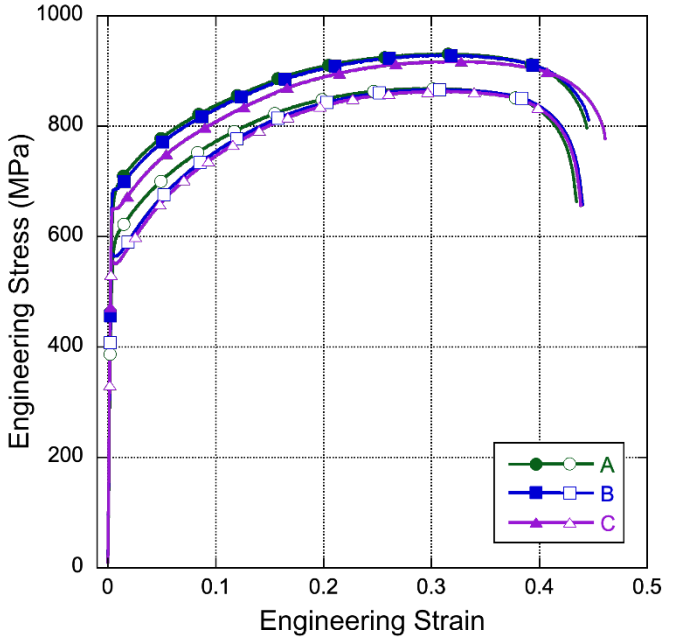

FIGURE 2: STRESS STRAIN CURVES OF XM-19 TUBING; OPEN SYMBOLS = NON-PRECHARGED (NP) AND CLOSED SYMBOLS = INTERNAL H (PC).

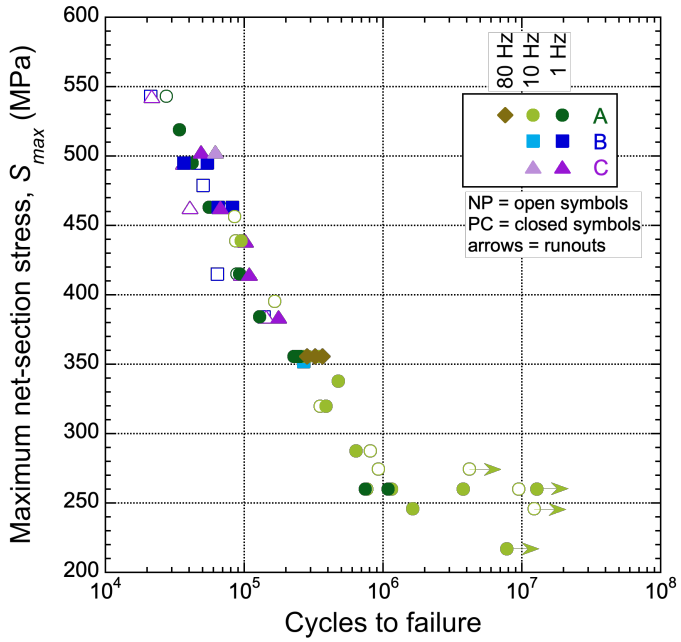

FIGURE 3: FATIGUE LIFE PLOT FOR XM-19 TUBING; OPEN SYMBOLS = NON-PRECHARGED (NP) AND CLOSED SYMBOLS = INTERNAL H (PC).

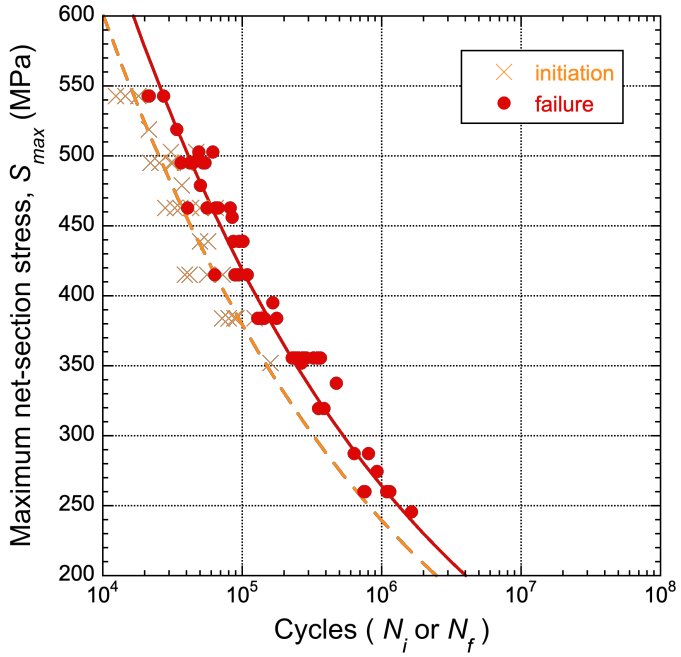

FIGURE 4: FATIGUE CRACK INITIATION AND FATIGUE LIFE FOR XM-19 TUBING. THE SOLID LINE REPRESENTS A POWER LAW FIT TO THE FAILURE DATA. THE DASHED LINE REPRESENTS THE CRACK INITIATION DATA, WHERE THE POWER-LAW EXPONENT IS ASSUMED TO BE IDENTICAL FOR INITIATION AND FAILURE.

3. RESULTS

Tensile testing

All tensile specimens failed in the middle of the gauge length. The basic tensile properties are summarized in Table 1 (average of at least two tests for each condition). Representative tensile flow curves are provided in Figure 2 for each condition both non-precharged (NP) and with internal H (PC, also referred to as H-precharged). The annealing steps had relatively little effect on the properties of the tubing; the strength properties varied by less than 10 MPa between the three heat-treated conditions (A, B, C) for each of the two environmental conditions, respectively (NP and PC); the total elongation varied by <1% between conditions A, B and C. In contrast, internal H increased the yield strength by about 20% and the tensile strength by 5-10%. The elongation was also slightly increased by internal H.

Fatigue testing

The cycles to failure (N_f) for all the tests are presented in Figure 3, plotted as the maximum net-section stress for the fatigue cycle (S_{max}). Runouts (specimens that did not fail) are indicated by arrows in the figure, whereas non-precharged (NP) and H-precharged (PC) tests are indicated by open and closed symbol, respectively. Based on the limited set of data, the measured fatigue life does not appear to depend on the thermal treatments, nor on internal H. All data (except for the runouts) can be represented by a single power law, fit with the cycles to failure as the dependent variable (i.e., opposite of the plotting convention). This fit is shown in Figure 4:

$$N_f = 1.29x10^{18}(S_{max})^{-5}$$

The cycles to crack initiation (N_i) are also shown in Figure 4. The crack initiation, likewise, is consistent across all tested conditions where crack initiation was monitored (typically S_{max} > 350 MPa), including all three heat treatments and both NP and PC environments. The crack initiation data can also be represented by a power law, with an exponent equal to the same value as determined for failure as shown in Figure 4 and can be represented as

$$N_i = 7.91x10^{17}(S_{max})^{-5}$$

The R values for the failure and initiation curve fits are >0.96 and >0.91, respectively.

4. DISCUSSION

Tensile properties

Internal H uniformly increases the tensile flow curve of the XM-19 tubing in this study (Figure 2), resulting in an increase in the tensile strength properties (yield and ultimate strength). This observation is consistent with previous reports in the literature for XM-19 and other austenitic stainless steels. The amount of strengthening due to internal H was shown to vary about linearly with hydrogen concentration for several other grades of austenitic stainless steel. Possible explanations for the origin of internal H strengthening are discussed in Ref. [13], but solid solution strengthening appears to be the likely explanation.

The elongation values are effectively unchanged by internal H in this study, perhaps even increased slightly. Previous studies have shown similar results for this and other austenitic stainless steels, although other ductility properties (e.g., reduction of area) and fracture resistance are clearly degraded by internal H. In other words, while simple tensile properties provide a relative assessment of a materials performance, tensile testing alone is insufficient to characterize more complex materials behavior, such as hydrogen-assisted fatigue and fracture.

Fatigue testing methodology

The fatigue testing method used in this study was previously demonstrated for type 316L tubing [2]. In the previous work, a fatigue frequency of 1 Hz was utilized. Here, longer duration tests were facilitated by testing at a higher frequency of 10 Hz, although most tests were performed at frequency of 1 Hz. Based on the limited testing, there was no systematic difference between tests at 1 and 10 Hz. Several tests were conducted at frequency of 80 Hz and also showed no significant change in the measured fatigue response as shown in Figure 3. This outcome is consistent with a study on the effect of strain rate in tensile testing with internal H [14], where the influence of strain rate was found to be similar for non-charged (NP) and H-precharged (PC) conditions respectively (in the range of 10^{-5} and 10^{-2} s^{-1}). In other words, the influence of internal H is not determined by strain rate, thus we might anticipate hydrogen-assisted fatigue (due to internal H) to be approximately insensitive to frequency in this range for a tensile-type configuration.

Testing at higher frequency is principally intended to improve testing throughput, not necessarily to manage hydrogen loss from the specimen. Although internal H will certainly diffuse out of the test specimen during handling and testing, significant loss of hydrogen requires much longer times than necessary to perform the tests, even for multi-day tests. For example, considering hydrogen diffusivity (D) in austenitic stainless steels at room temperature of ~10^{-16} m^2/s [15], a simple estimate of hydrogen diffusion distance using $L \sim (4Dt)^{1/2}$ (where t is time), suggests a small diffusion distance of about 0.02 mm over 5 days, compared to the tubing wall thickness of 1.2 mm. In other words, very little hydrogen is expected to be lost over the time scale of the tests in this study.

In summary, fatigue life testing of tube specimens with a cross hole has been shown to provide typical power-law response expected of stress-controlled fatigue testing. Moreover, the results appear to be insensitive to frequency in the range of 1 to 80 Hz. This latter observation is consistent with expectations based on known strain rate effects in austenitic stainless steels and the rate of hydrogen diffusion.

Fatigue life response

The fatigue life performance of annealed XM-19 tubing is not affected by internal H for the configuration in this study. Annealing cycles (of 1050˚C) also do not seem to influence the

fatigue response, nor change the response to internal H (Figure 3). In contrast, fatigue testing of type 316L tubing in the same configuration with internal H was reported to decrease the cycles to failure and the cycles to crack initiation [2], although very modestly. Thus, we can conclude that the fatigue life performance of XM-19 is superior to the performance of type 316L, likely a consequence of the higher strength of XM-19.

Fatigue crack initiation

The similitude between the crack initiation and failure responses allows the data to be fit by power laws with the same exponent. Consequently, the number of cycles to crack initiation must then be a constant fraction of the cycles to failure for all stresses (where the power laws represent the data). Moreover, since the data for NP and PC environments are indistinguishable, crack initiation appears to be unaffected by internal H. For these data (all conditions), crack initiation occurs at about 60% of the cycles to failure. In contrast, measurements for type 316 from Ref. [2] found crack initiation occurred at less than 50% of the cycles to failure. This difference may be reflective of the inferior fatigue response of the type 316L and the lower strength.

5. SUMMARY

The effects of internal H on the mechanical properties of XM-19 tubing were evaluated. The tensile elongation of the tubing was slightly increased in most cases with internal H, while the strength properties were increased by as much as 20% consistent with other austenitic stainless steels. The fatigue life of XM-19 tubing was explored by axially loading a section of tubing with a cross hole to induce a stress concentration in the middle of the length of tubing. The fatigue life of the annealed tubing appears to be unaffected by high concentration of internal H. Additional annealing steps also did not change the fatigue response of the tubing with or with internal H. Crack initiation was probed with the DCPD method. The cycles to crack initiation could be estimated as a constant fraction of the cycles to failure over the entire evaluated stress range (namely for peak applied fatigue stresses from about 350 to 550 MPa).

ACKNOWLEDGEMENTS

This article has been authored by an employee of National Technology & Engineering Solutions of Sandia, LLC under Contract No. DE-NA0003525 with the U.S. Department of Energy (DOE). The employee owns all right, title and interest in and to the article and is solely responsible for its contents. The United States Government retains and the publisher, by accepting the article for publication, acknowledges that the United States Government retains a non-exclusive, paid-up, irrevocable, world-wide license to publish or reproduce the published form of this article or allow others to do so, for United States Government purposes. The DOE will provide public access to these results of federally sponsored research in accordance with the DOE Public Access Plan https://www.energy.gov/downloads/doe-public-access-plan.

This paper describes objective technical results and analysis. Any subjective views or opinions that might be expressed in the paper do not necessarily represent the views of the U.S. Department of Energy or the United States Government.

REFERENCES

[1] T. Michler, Y. Lee, R. P. Gangloff, and J. Naumann, "Influence of macro segregation on hydrogen environment embrittlement of SUS 316L stainless steel," *Int J Hydrogen Energy* 34 (2009) 3201-3209.

[2] B. Kagay, C. San Marchi, V. Pericoli, and J. Foulk III, "Hydrogen effects on fatigue life of welded austenitic stainless steels evaluated with hole-drilled tubular specimens " in *Proceedings of the ASME 2020 Pressure Vessels and Piping Division Conference*, Online, 19-24 July 2020 2020: ASME.

[3] C. San Marchi, B. P. Somerday, X. Tang, and G. H. Schiroky, "Effects of alloy composition and strain hardening on tensile fracture of hydrogen-precharged type 316 stainless steels," *Int J Hydrogen Energy* 33 (2007) 889-904.

[4] C. San Marchi, T. Michler, K. A. Nibur, and B. P. Somerday, "On the physical differences between tensile testing of type 304 and 316 austenitic stainless steels with internal hydrogen and in external hydrogen," *Int J Hydrogen Energy* 35 (2010) 9736-9745.

[5] B. C. Odegard and A. J. West, "On the Thermo-Mechanical Behavior and Hydrogen Compatibility of 22-13-5 Stainless Steel," *Mater Sci Eng* 19 (1975) 261-270.

[6] G. R. Caskey, "Hydrogen Compatibility Handbook for Stainless Steels (DP-1643)," EI du Pont Nemours, Savannah River Laboratory, Aiken SC, DP-1643, June 1983.

[7] G. R. Caskey, "Hydrogen Effects in Stainless Steels," in *Hydrogen Degradation of Ferrous Alloys*, R. A. Oriani, J. P. Hirth, and M. Smialowski Eds. Park Ridge NJ: Noyes Publications, 1985, pp. 822-862.

[8] C. San Marchi, D. K. Balch, K. Nibur, and B. P. Somerday, "Effect of high-pressure hydrogen gas on fracture of austenitic steels," *J Pressure Vessel Technol* 130 (2008) 041401.

[9] K. A. Nibur, B. P. Somerday, C. San Marchi, and D. K. Balch, "Effects of strength and microstructure on hydrogen-assisted crack propagation in 22Cr-13Ni-5Mn stainless steel forgings," *Metall Mater Trans* 41A (2010) 3348-3357.

[10] C. San Marchi and B. P. Somerday, "Technical Reference on Hydrogen Compatibility of Materials (SAND2012-7321)," Sandia National Laboratories, Livermore CA, 2012.

[11] C. San Marchi, B. Somerday, and K. A. Nibur, "Fatigue crack initiation in hydrogen-precharged austenitic stainless steel," in *2012 International Hydrogen*

Conference, Moran WY, B. P. Somerday and P. Sofronis, Eds., 9-12 September 2012 2012: ASME.

[12] K. A. Nibur, P. J. Gibbs, J. W. Foulk, and C. S. Marchi, "Notched fatigue of austenitic alloys in gaseous hydrogen (PVP2017-65978)," in *Proceedings of PVP-2017: ASME Pressure Vessels and Piping Division Conference*, Waikoloa HI, 2017: ASME.

[13] C. San Marchi, B. P. Somerday, X. Tang, and G. H. Schiroky, "Hydrogen-assisted fracture of type 316 stainless steel at subambient temperature (PVP2008-61240)," in *Proceedings of PVP-2008: ASME Pressure Vessels and Piping Division Conference*, Chicago IL, July 27-31, 2008 2008: ASME, pp. PVP2008-61240.

[14] R. W. Wheeler III, J. Ronevich, C. San Marchi, J. W. Foulk, M. Diab, and C. Alleman, "Combined hydrogen embrittlment and strain rate sensitivity of annealed and forged 304L steel," in *ASME Pressure Vessels and Piping (PVP) Conference* Atlanta GA, 16-21 July 2023 2023: ASME.

[15] C. San Marchi, B. P. Somerday, and S. L. Robinson, "Permeability, Solubility and Diffusivity of Hydrogen Isotopes in Stainless Steels at High Gas Pressure," *Int J Hydrogen Energy* 32 (2007) 100-116.

TABLE 1: COMPOSITION (WT%) OF THE XM-19 AUSTENITIC STAINLESS STEEL TUBING.

Fe	Cr	Ni	Mn	Mo	Nb	V	Si	C	N	S	P
Bal	22.0	13.1	5.3	2.1	0.20	0.20	0.35	0.015	0.32	0.001	0.016

TABLE 2: TENSILE PROPERTIES OF THE XM-19 AUSTENITIC STAINLESS STEEL TUBING. ALL VALUES ARE THE AVERAGE OF AT LEAST TWO TESTS.

Condition	Environment	Sy (MPa)	Su (MPa)	Elu (%)	Elt (%)
A	NP	566	872	29.3	43.4
	PC	692	939	29.9	43.0
B	NP	569	870	30.2	44.0
	PC	674	924	31.2	45.2
C	NP	561	864	30.7	43.9
	PC	586	895	33.2	47.0

NP = not precharged; PC = H-precharged (internal H)